# *GALC* gene is downregulated by promoter hypermethylation in Epstein-Barr virus-associated nasopharyngeal carcinoma

YINGHAI ZHAO[1], YING GUO[1], ZHIJING WANG[1], ZEBIN XIAO[1], RONG LI[2], AIHUA LUO[3], CHANGLI WU[4], ZHILIANG JING[1], NING SUN[1], XIAOYI CHEN[1], HAIJUN DU[5] and YI ZENG[5]

Departments of [1]Pathology and [2]Pathophysiology, Guangdong Medical University, Zhanjiang, Guangdong 524023; [3]Department of Pathology, Gaozhou People's Hospital, Gaozhou, Guangdong 525200; [4]Department of Physiology, Guangdong Medical University, Zhanjiang, Guangdong 524023; [5]National Institute for Viral Disease Control and Prevention, Chinese Center for Disease Prevention and Control, State Key Laboratory for Infectious Disease Prevention and Control, Beijing 100052, P.R. China

Received April 3, 2015; Accepted July 2, 2015

DOI: 10.3892/or.2015.4134

**Abstract.** The aim of the study was to investigate the tumor-suppressor effect of *GALC* in Epstein-Barr virus (EBV)-associated nasopharyngeal carcinoma (NPC) and determine whether *GALC* was downregulated by promoter hypermethylation in the NPC cell line, CNE-2Z. Forty-one archival NPC biopsy specimens were compared with 15 chronic nasopharyngitis specimens. EBV-encoded RNA (EBER) was verified by *in situ* hybridization and GALC protein expression was analyzed by immunohistochemistry. Promoter methylation in CNE-2Z cells was analyzed by bisulfite sequencing polymerase chain reaction. The functional role of GALC in NPC was investigated by restoring GALC expression in CNE-2Z cells via treatment with the DNA-demethylating agent 5-Aza-2'-deoxycytidine (5-Aza-dC). EBER was expressed in 92.68% NPC specimens but no chronic nasopharyngitis specimens (P<0.01). GALC protein was present in 60% of chronic nasopharyngitis specimens and 24.39% NPC specimens (P<0.05). GALC protein expression was present significantly more frequently in tumors without lymph node metastasis than in those with metastasis (P<0.05). Logistic regression showed that GALC protein expression protected against lymph node metastasis (P<0.05). GALC protein expression was not correlated with age, gender and TNM stage (P>0.05). Treatment of GALC-negative CNE-2Z cells with 5-Aza-dC reduced *GALC* promoter methylation and restored GALC expression in a dose-dependent manner (P<0.05). The re-expression of GALC in CNE-2Z cells reduced cell proliferation and migration compared to the controls (P<0.05). *GALC* was downregulated by promoter hypermethylation and contributed to the pathogenesis of EBV-associated NPC. The findings showed the putative tumor-suppressor effect of GALC in NPC.

*Correspondence to:* Professor Xiaoyi Chen, Department of Pathology, Guangdong Medical University, No. 57 Renming South Road, Zhanjiang, Guangdong 524023, P.R. China
E-mail: 13692490452@139.com

*Abbreviations:* NPC, nasopharyngeal carcinoma; EBV, Epstein-Barr virus; EBER, Epstein-Barr virus-encoded RNA; 5-Aza-dC, 5-Aza-2'-deoxycytidine; GALC, galactocerebrosidase; LMP, latent membrane protein; EBNA, EBV nuclear antigen; BARTs, *Bam*HI A rightward transcripts; LOH, loss of heterozygosity

*Key words:* nasopharyngeal neoplasm, galactocerebrosidase, Epstein-Barr virus, epigenetics, methylation, proliferation, migration

## Introduction

Nasopharyngeal carcinoma (NPC) is a human epithelial malignancy with high incidence in southern China, particularly, in the Cantonese population. The Epstein-Barr virus (EBV) was the first human tumor virus to be identified and has yielded significant insights into the pathogenesis of cancer. Latent EBV infection is one of the most important factors for NPC in endemic areas. NPC is associated with EBV latent infection type II and the expression of EBV latent membrane protein (LMP) 1, EBV-LMP2A, EBV-LMP2B, EBV nuclear antigen (EBNA) 1, EBV-encoded RNA (EBER) 1, EBER2 and the *Bam*HI A rightward transcripts (BARTs) (1-3). Metastasis to the neck lymph nodes is the predominant initial symptom in NPC. In addition, recurrence and distant metastasis after radiotherapy are known to occur in NPC. Therefore, it is imperative to identify novel diagnostic and therapeutic approaches.

Loss of heterozygosity (LOH) on chromosomes 13q and 14q are common genetic events, and putative tumor-suppressor genes located in these regions may be involved in the development of NPC (4,5). Evidence from LOH studies showed that NPC-related tumor-suppressor genes may be present at 14q24-q32 (5). LOH on chromosome 14q was detected in 80% of NPC tumors with high-frequency LOH loci clustered to 14q11-q13, 14q21-q24 and 14q32 (5). The *GALC* gene is located at 14q31, has 17 exons and 16 introns of an approximate size of 60 kb (6). Aberrant methylation in the promoters of tumor-related genes is closely associated with epigenetically mediated gene silencing (7-14). DNA hypermethylation in the promoter region has been reported in NPC (7-10). Hypermethylation of the 9p21 chromosomal region genes (p14, p15 and p16) has been observed in the peripheral blood

of leukemic patients (11). DNA methylation in cancer-related genes can be a potential biomarker and therapeutic target for prostate cancer (12). It has been reported that p16 promoter methylation is a promising potential biomarker for the early diagnosis of gastric cancer (13). A potential biomarker panel assessing the hypermethylation of six gene promoters holds great promise as a diagnostic test for high-grade (type II) serous ovarian cancer (14).

Therefore, we aimed to investigate the possible tumor-suppressor effect of the *GALC* gene in EBV-associated NPC, and identified that the *GALC* gene is downregulated by promoter hypermethylation in the NPC cell line, CNE-2Z.

## Materials and methods

*Specimens*. The World Health Organization has classified NPC into different histological types [keratinizing squamous cell carcinoma (type I), differentiated non-keratinizing carcinoma (type II) and undifferentiated non-keratinizing carcinoma (type III)] based on the tumor cell appearance on light microscopy (15). Type II and III NPC are predominantly EBV-positive.

Specimens of type III NPC and chronic nasopharyngitis were obtained from patients diagnosed with these conditions between January 2008 and August 2012 at the Affiliated Hospital of Guangdong Medical College and Gaozhou People's Hospital (Guangdong, China). Informed consent was obtained from all the participants. None of the NPC patients were previously treated with radiotherapy or chemotherapy. Of the 41 NPC patients whose specimens were used for immunohistochemical analysis, 7 were at TNM stage II, 21 were at stage III and 13 were at stage IV. There were 35 men and 6 women in the NPC group, with ages ranging from 31 to 86 years (median age, 54 years; mean age, 52 years). Of the 15 chronic nasopharyngitis patients, 9 were male and 6 were female, with ages ranging from 15 to 79 years (median age, 47 years; mean age, 45.9 years).

*EBER in situ hybridization*. The sections of 41 NPC tumor specimens were dewaxed in xylene and digested with proteinase K for 16 min. The sections were then rehydrated in serial graded ethanol washes (70, 95 and 100%) and hybridized for 2 h at 37˚C with digoxigenin-labeled EBER probes (ZSGB-BIO, China). The hybridization products were detected using anti-digoxigenin-horseradish peroxidase (ZSGB-BIO, Beijing, China) for 30 min at 37˚C, followed by 3 min of incubation in diaminobenzidine solution for the detection of EBERs. The slides were counterstained with Mayer's hematoxylin and positive staining was observed as brown granules at the site of hybridization on light microscopy. Only specimens with signals within the tumor cell nuclei were considered to be positive.

*Immunohistochemical staining*. Tissue samples were fixed in 10% buffered formalin, dehydrated, embedded in paraffin and cut into 4-$\mu$m sections. The samples were evaluated by two experienced pathologists. Sections with known high and no GALC expression were used as positive and negative controls, respectively. The sections incubated with 0.01 mol/l phosphate-buffered saline (PBS) instead of primary antibody served as the blank control. A streptavidin-peroxidase (SP) kit was purchased from Beijing Zhongshan Golden Bridge Biotechnology, Co. (Beijing, China). Rabbit anti-human GALC polyclonal antibody was purchased from the Proteintech Group, Inc. (Chicago, IL, USA) (working dilution, 1:200). Procedures were implemented according to the manufacturer's instructions.

*Evaluation of in situ hybridization and immunohistochemical staining*. For each section, five low magnification fields (x100) were randomly selected under a microscope, and the proportions of positively stained cells per field were determined under higher magnification (x400). The results were expressed as the mean percentage of positively stained cells in the five fields. GALC was specifically located in the cytoplasm. The staining intensity (A) was classified as follows: negative, 0 points; weak, 1 point; moderate, 2 points; and strong, 3 points. The percentage of positive cells (B) was classified as: 0%, 0 points; 1-25%, 1 point; 26-50%, 2 points; 51-75%, 3 points, and >75%, 4 points. The product of A and B yielded the final score, which was classified as follows: 0-1, negative (-) and ≥2, positive (+). The sections were evaluated by three pathologists who were blinded to the study design.

*Cell culture and drug treatment*. The NPC CNE-2Z cell line which has low differentiation, was obtained from the Department of Pathology, Guangdong Medical College. The CNE-2Z cells were cultured in RPMI-1640 with 10% fetal bovine serum (FBS; HyClone, Laboratories, Logan, UT, USA), 0.1 $\mu$M penicillin and 0.1 $\mu$M streptomycin under 5% $CO_2$ at 37˚C. For drug treatment, exponentially growing CNE-2Z cells were seeded at a density of $2x10^5$ cells/well into 6-well plates. The cells were treated with different doses (0, 5, 10, 20, 40 and 60 $\mu$M/l) of the demethylation agent 5-Aza-2'-deoxycytidine (5-Aza-dC; Sigma, St. Louis, MO, USA) for 48 h. The cells were collected for the detection of GALC protein expression using western blotting and immunofluorescent assay, *GALC* mRNA expression using reverse transcriptase-polymerase chain reaction (RT-PCR) assay, *GALC* gene promoter methylation using bisulfite sequencing PCR (BSP), cell proliferation using Cell Counting kit (CCK)-8 assay, and cell migration using scratch and Transwell migration assays.

*Quantitative RT-PCR*. Total RNA was extracted from the cultured CNE-2Z cells using RNAiso Plus (Takara, Japan). Reverse transcription was performed with the PrimeScript™ RT reagent kit (Takara). The primers used for the PCR assay were: *GALC*, 5'-AGGGAACCTCACCATCATCA-3' (forward) and 5'-GCTGTCAAGGAGCCATAGAGAA-3' (reverse); and GAPDH, 5'-AGGTCGGAGTCAACGGATTTG-3' (forward) and 5'-GTGATGGCATGGACTGTGGT-3' (reverse). PCR was performed in a LightCycler 480 fluorescent quantization PCR thermal cycler (Roche, Switzerland). Quantitative RT-PCR was performed with SYBR® Premix Ex *Taq*™ II (Takara) at 95˚C for 30 sec, followed by 40 cycles of 95˚C for 5 sec and 60˚C for 30 sec, after which a melt-curve analysis was performed once from 60 to 95˚C, followed by 1 cycle at 50˚C for 30 sec. The level of GAPDH mRNA was used as an internal control. The reactions were performed in triplicate. The relative amounts of *GALC* mRNA were calculated in accordance with the $2^{-\Delta\Delta Ct}$ method.

*BSP*. Bisulfite modification of genomic DNA converts unmethylated deoxycytidine to uracil (read as thymidine), however, methylated deoxycytidine remained unmodified. A 372-bp region within the promoter (-158 to +214 nucleotides relative to the transcriptional start site) containing the CpG island was PCR-amplified from the bisulfite-treated DNA. The PCR fragments were cloned and sequenced in 10 clones, thereby allowing identification of the methylation status of each of the 37 specific CpG sites in the *GALC* gene. The methylation primers of the *GALC* gene promoter region used for the BSP assay were: 5'-TTG(T/C)GTTAAAGTGTTTTATTA GGTGA-3' (forward) and 5'-CAAC(A/G)CACACAACAAC AAAAACA-3' (reverse).

*Western blot analysis*. Total cellular proteins of the harvested CNE-2Z cells were extracted. The standard western blotting protocol was applied. The specific primary antibody anti-GALC (working dilution, 1:200; Proteintech) and a horseradish peroxidase-conjugated secondary antibody (Mai Bio Co., Ltd, Zhejiang, China) were used. Specific bands were visualized using enhanced chemiluminescence reagents and recorded on film.

*Immunofluorescent staining*. CNE-2Z cells were fixed in 4% paraformaldehyde for 15 min at room temperature, blocked and incubated with the primary antibody anti-GALC (working dilution, 1:200), the secondary antibody Rhodamine-conjugated goat anti-rabbit IgG (both from Proteintech) and 4',6-diamidino-2-phenylindole (DAPI; Sigma). In each experiment, the immunopositive cells in five randomly selected fields were counted and 500-1,000 cells were counted in total.

*Cell viability*. The proliferation of CNE-2Z cells was determined using the CCK-8 assay, according to the manufacturer's instructions (Beyotime Institute of Biotechnology, Shanghai, China). Exponentially growing CNE-2Z cells ($4x10^3$ cells/well) in 100 $\mu$l medium were seeded in 96-well plates. After 12 h, the medium in each well was replaced with media containing different concentrations of 5-Aza-dC (0, 5, 10, 20, 40 and 60 $\mu$M/l), and the plates were incubated for 48 h. The supernatant was removed, and 200 $\mu$l of CCK-8 and RPMI-1640 mixed medium was added into each well, followed by incubation for 2 h at 37˚C in the dark. The absorbance of CCK-8-containing medium was measured at a wavelength of 450 nm (reference wavelength, 630 nm) using a microplate reader (Bio-Rad, Hercules, CA, USA). Cell proliferation was calculated as: Viability = $(OD_{test\ group}p - OD_{blank\ group})/(OD_{control\ group} - OD_{blank\ group})$. The results were presented as mean ± standard deviation (SD). Three independent experiments, each in triplicate, were conducted.

*Cell migration*. *In vitro* scratch and Transwell chamber assays were performed to assess the migration of CNE-2Z cells. Exponentially growing CNE-2Z cells ($8x10^5$ cells/well) were seeded in 6-well plates. When the cells were cultured to 90% confluency, each well was manually scratched three times with a 200-$\mu$l pipette tip, washed with PBS three times and incubated at 37˚C with media containing different concentrations of 5-Aza-dC (0, 20 and 40 $\mu$M/l). Cell images were recorded at 0 and 24 h. The distance between two cell edges was analyzed using Image-Pro software.

The Transwell system (24 wells, 8-$\mu$m pore size with polycarbonate membrane; Corning Costar, NY, USA) not coated with Matrigel was used for the migration assay. The CNE-2Z cells were incubated with media containing different concentrations of 5-Aza-dC (0, 20 and 40 $\mu$M/l) at 37˚C for 48 h. A total of $4x10^4$ cells were suspended in 100 $\mu$l serum-free medium and were seeded in the upper chambers. Then, 600 $\mu$l RPMI-1640 containing 10% FBS was added to the lower chamber. After 24 h, the cells remaining in the upper chambers were removed with a cotton swab, while the cells attached to the lower surface were fixed with methanol and stained with hematoxylin and eosin (H&E). The cells migrating to the lower side in five randomly selected fields were counted by light microscopy, and the total number of migrating cells was determined and analyzed statistically. Each experiment was performed in triplicate.

*Statistical analysis*. Statistical analyses were performed using SPSS 17.0. One-way analysis of variance (ANOVA) was performed to analyze the data from the CCK-8, scratch and Transwell chamber assays and RT-PCR. The $\chi^2$ and the Fisher's exact tests, and the logistic regression analysis were used to compare the rates between the different groups and to test the correlation between two factors. P<0.05 was considered to indicate a statistically significant result.

Table I. EBER and GALC protein expression in the columnar epithelium of the nasopharyngeal mucosa and in NPC.

| | | EBER[a] | | GALC[b] | |
|---|---|---|---|---|---|
| Groups | n | - | + (%) | - | + (%) |
| Nasopharyngeal mucosal columnar epithelium | 15 | 15 | 0 (0) | 6 | 9 (60.00) |
| NPC cells | 41 | 3 | 38 (92.68) | 31 | 10 (24.39) |

[a]Fisher's exact test, P<0.01. [b]$\chi 2$=6.212, P<0.05. EBER, EBV-encoded RNA; NPC, nasopharyngeal carcinoma.

## Results

*EBER and GALC protein expression in chronic nasopharyngitis and NPC*. A high expression of EBER was detected in the specimens from the 41 NPC patients. EBER expression was not correlated with different clinicopathological parameters, such as age, gender, lymph node metastasis and TNM stage (P>0.05).

*EBER and GALC protein expression in the columnar epithelium of the nasopharyngeal mucosa and in NPC*. No EBER expression was found in the columnar epithelial of the nasopharyngeal mucosa obtained from the 15 individuals in the control group. By contrast, 92.68% of the NPC specimens

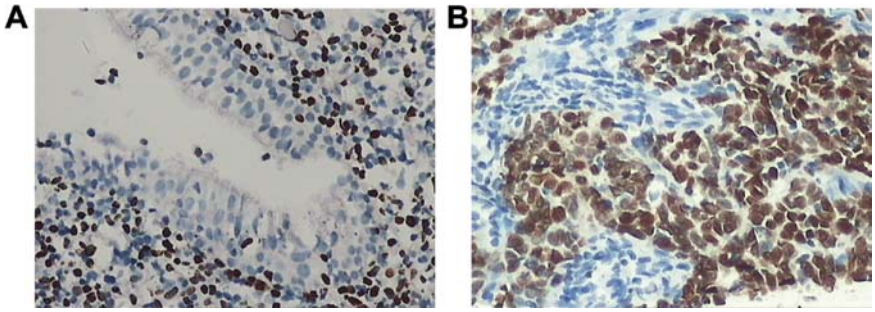


Figure 1. (A) Nasopharyngeal mucosal columnar epithelia show no *in situ* hybridization signals of EBV-encoded RNA. However, lymphocytes showing dark brown *in situ* hybridization signals of EBV-encoded RNA (magnification, x200). (B) NPC cells show dark brown *in situ* hybridization signals of EBV-encoded RNA (magnification, x200). EBV, Epstein-Barr virus; NPC, nasopharyngeal carcinoma.

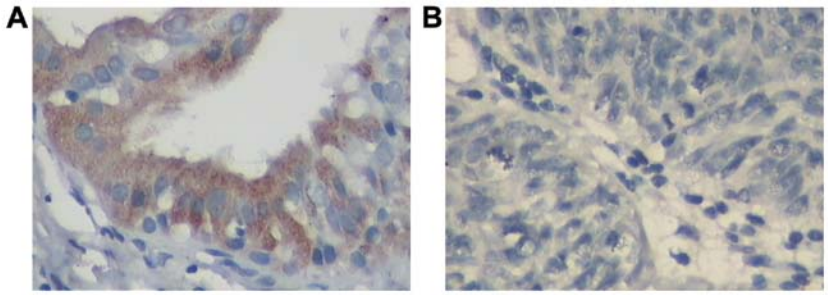


Figure 2. *GALC* protein expression in chronic nasopharyngitis and NPC. The expression of GALC protein was detected in all the samples following immunohistochemical staining. For *GALC*, cytoplasmic staining was considered positive. The image shows two specimens with positive and negative staining. (A) *GALC* protein expression is observed in nasopharyngeal mucosal columnar epithelium (magnification, x400). (B) *GALC* protein expression is negative in NPC cells (magnification, x400). NPC, nasopharyngeal carcinoma.

from the 41 NPC patients exhibited EBER expression. The immunohistochemical SP method was used to measure the expression of GALC protein. GALC protein expression was detected in 24.39% of NPC specimens, which had a high rate of EBV latent infection. GALC protein expression was detected in 60.00% of columnar epithelia of chronic nasopharyngitis specimens with no EBV latent infection. The difference between these two groups was statistically significant (P<0.05) (Table I).

*Relationship between GALC protein expression and clinicopathological parameters of NPC*. The *GALC* protein expression was not correlated with age, gender and TNM stage (P>0.05) (Table II). GALC protein expression occurred significantly more frequently in tumors without lymph node metastasis than in tumors with metastasis (P<0.05) (Table II). Logistic regression showed that GALC protein expression protected against lymph node metastasis (P<0.05) (Table III).

*Effect of different 5-Aza-dC concentrations on GALC gene methylation status of CNE-2Z cells*. To confirm that hypermethylation of the 37 CpG sites in the promoter region (-158 to +214) of the *GALC* gene decreased after 5-Aza-dC treatment, CNE-2Z cells were treated with different concentrations of 5-Aza-dC (0, 5, 10, 20, 40 and 60 $\mu$M/l) for 48 h, and the methylation status of the *GALC* gene promoter was analyzed using bisulfite genomic sequencing in the control (0 $\mu$M/l) and treated samples (Fig. 3). In the control sample, CpG sites were 95.9% methylated, and in the treated samples the sites were 86.5, 81.9, 50.8, 71.6 and 70.3% methylated at the concentrations of 5, 10, 20, 40 and 60 $\mu$M/l, respectively.

Table II. Relationship between GALC protein expression and clinicopathological parameters in NPC.

| Clinicopathological parameters | GALC | | | P-value |
|---|---|---|---|---|
| | n | - | + (%) | |
| Age (years) | | | | |
| <40 | 5 | 5 | 0 (0) | 0.31 |
| ≥40 | 36 | 26 | 10 (27.77) | |
| Gender | | | | |
| Male | 35 | 26 | 9 (25.71) | 1 |
| Female | 6 | 5 | 1 (16.66) | |
| Lymph node metastasis | | | | |
| No | 12 | 6 | 6 (50.00) | 0.040[a] |
| Yes | 29 | 25 | 4 (13.79) | |
| TNM stage | | | | |
| II | 7 | 3 | 4 (57.14) | 0.083 |
| III | 21 | 17 | 4 (19.04) | |
| IV | 13 | 11 | 2 (15.38) | |

[a]Statistically significant. NPC, nasopharyngeal carcinoma.

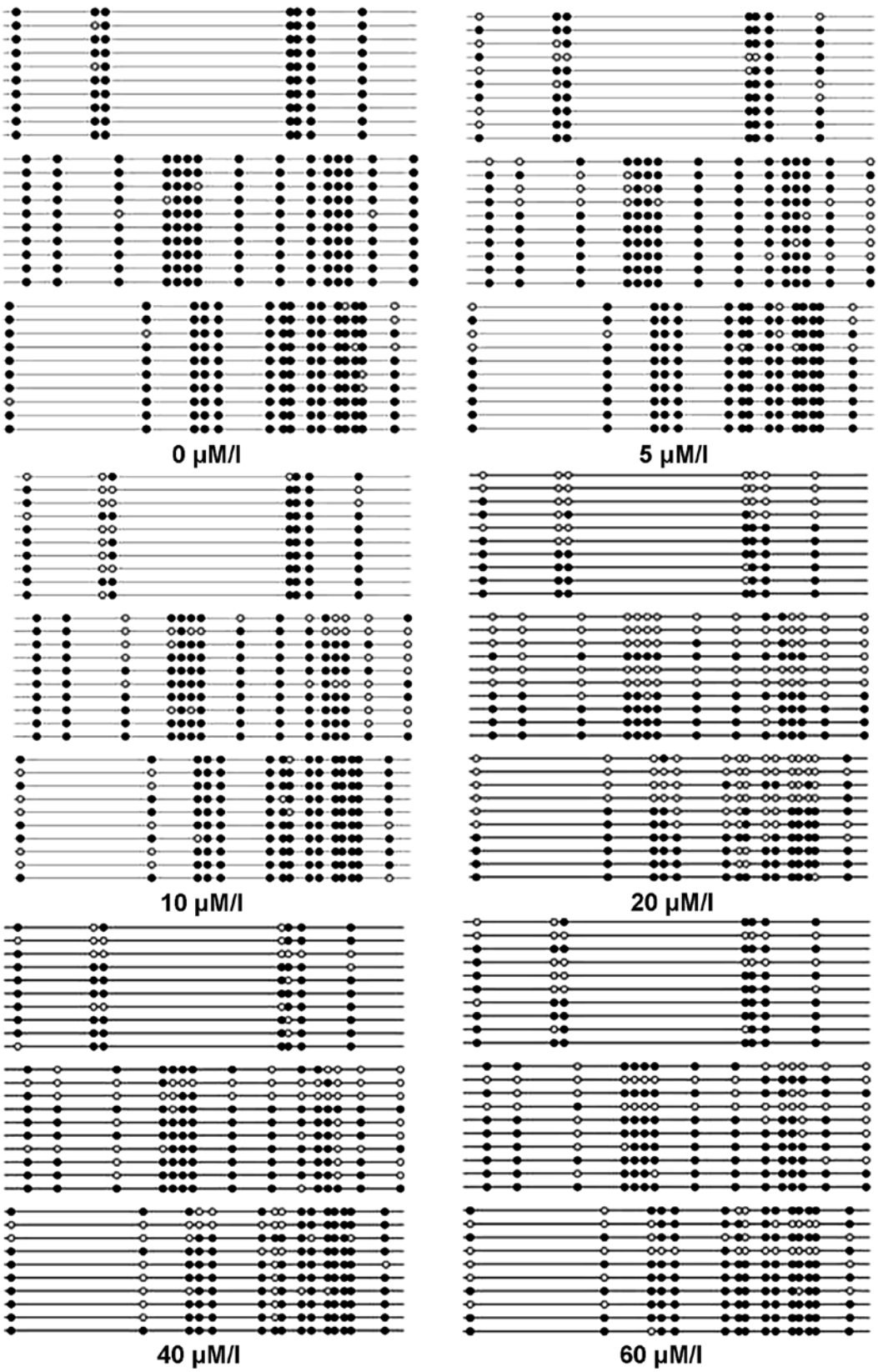


Figure 3. Methylation status of the *GALC* gene promoter region in CNE-2Z cells treated with different concentrations of 5-Aza-dC (0, 5, 10, 20, 40 and 60 $\mu$M/l) for 48 h. The methylation status of the 37 CpG sites of the *GALC* gene promoter region is shown. (○, unmethylated CpG site; ●, methylated CpG site). 5-Aza-dC, 5-Aza-2'-deoxycytidine.

*Effect of different concentrations of 5-Aza-dC on GALC mRNA expression in CNE-2Z cells*. To provide evidence for a possible role of DNA methylation in the regulation of *GALC* expression, we analyzed *GALC* mRNA levels in CNE-2Z cells using RT-PCR in the control and treated groups (Fig. 4). The results showed that *GALC* mRNA levels were significantly

Table III. Logistic regression analysis of GALC protein expression and lymph node metastasis in NPC (n=41).

| Selected factor | β | SE | Wald | P-value | Exp (β) | 95% CI |
|---|---|---|---|---|---|---|
| GALC | -1.8326 | 0.7895 | 5.3877 | 0.020 | 0.160 | 0.034-0.752 |

CI, confidence interval; NPC, nasopharyngeal carcinoma.

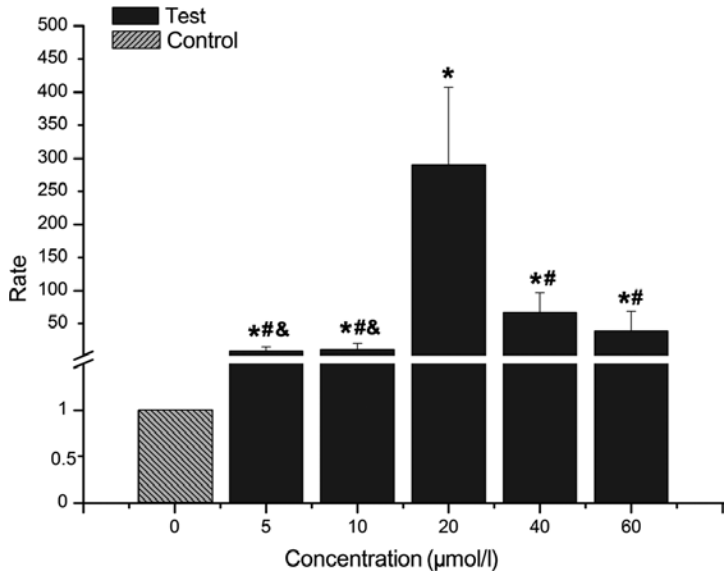


Figure 4. *GALC* mRNA expression detected using RT-PCR analysis. The control sample and the CNE-2Z cells were treated with different concentrations of 5-Aza-dC (5, 10, 20, 40 and 60 $\mu$M/l) for 48 h, and then subjected to RT-PCR to analyze the *GALC* mRNA expression levels. The *GALC* mRNA expression levels in the treated samples (20, 40 and 60 $\mu$M/l) significantly differed from those in the control samples. Statistical analysis was performed using one-way ANOVA, followed by the significant difference (Dunnett's T3) test. Data are presented as means ± SD, n=3. $^{*}$P<0.05, treated groups vs. control. $^{\#}$P<0.01, 5, 10, 40 and 60 $\mu$M/l vs. 20 $\mu$M/l. $^{\&}$P<0.05, 5 and 10 $\mu$M/l vs. 40 $\mu$M/l. 5-Aza-dC, 5-Aza-2'-deoxycytidine.

higher in the treated groups than those in the control group (P<0.05). *GALC* mRNA levels in the 5, 10, 40 and 60 $\mu$M/l groups were significantly lower than that in the 20 $\mu$M/l group (P<0.01), while the levels in the 5 and 10 $\mu$M/l groups were significantly lower than that in the 40 $\mu$M/l group (P<0.05). *GALC* mRNA levels in the 5, 10 and 40 $\mu$M/l groups did not significantly differ from that in the 60 $\mu$M/l group (P>0.05).

*GALC protein expression in CNE-2Z cells treated with different concentrations of 5-Aza-dC and detected using western blotting and immunofluorescence*. To provide evidence for a possible role of DNA methylation in the regulation of *GALC* expression, we analyzed GALC protein expression using western blotting and immunofluorescence analyses before and after treatment with different concentrations of 5-Aza-dC (5, 10, 20, 40 and 60 $\mu$M/l) for 48 h (Fig. 5). The results showed that *GALC* protein expression was absent in the control group but present in the cells treated with 5-Aza-dC. GALC protein expression was highest in the 20 $\mu$M/l group.

These results indicated a correlation between the methylation status of the *GALC* gene and the expression level of *GALC* mRNA or protein. Data suggest that promoter methylation suppresses *GALC* gene expression, and 5-Aza-dC-induced demethylation of CpG sites upregulates *GALC* gene expression in the NPC CNE-2Z cell line.

*Effect of different concentrations of 5-Aza-dC on CNE-2Z cell proliferation*. CCK-8 was used to examine the proliferation of CNE-2Z cells treated with different concentrations of 5-Aza-dC for 48 h (Fig. 6). The results showed that cell viability was significantly decrased in the 20, 40 and 60 $\mu$M/l groups than in the control group (P<0.05). The cell viability in the 5 and 10 $\mu$M/l groups significantly differed from that in the 20 $\mu$M/l group (P<0.05), while in the 5, 10 and 40 $\mu$M/l groups cell viability significantly differed from that in the 60 $\mu$M/l group (P<0.05). The viability in the 40 and 60 $\mu$M/l groups did not significantly differ from that the in 20 $\mu$M/l group (P>0.05).

*Cell migration and scratch assay*. After the CNE-2Z cells were treated with 20 or 40 $\mu$M/l 5-Aza-dC for 24 h, the relative cell migration distance was significantly higher in the treatment group than in the control group. Moreover, the cell migration ability decreased with an increasing concentration of 5-Aza-dC, and the differences between the treatment and control groups were statistically significant (P<0.01). However, no significant difference was found between the 20 and 40 $\mu$M/l group (P>0.05; Fig. 7).

*Cell migration and Transwell chamber assay*. After the CNE-2Z cells were treated with 20 or 40 $\mu$M/l 5-Aza-dC

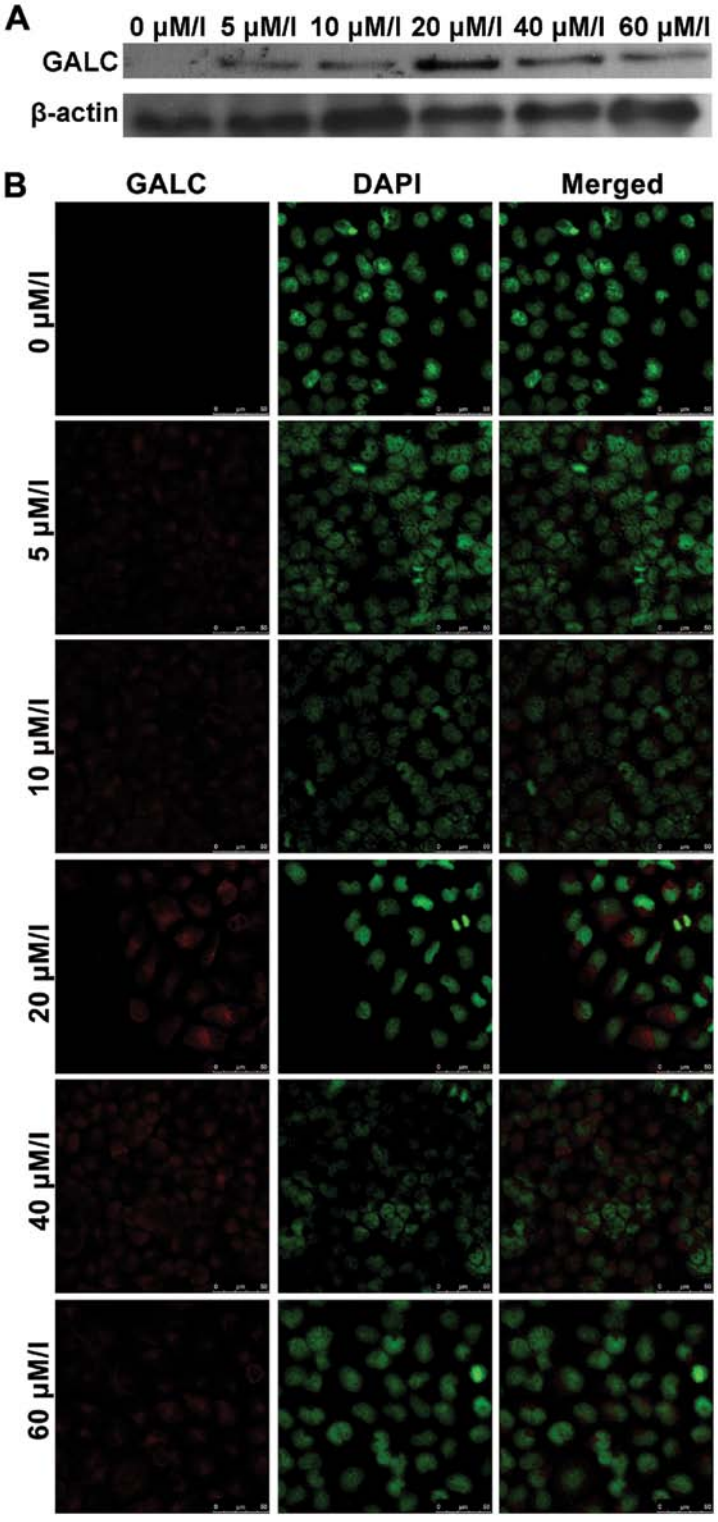


Figure 5. *GALC* protein expression in CNE-2Z cells was analyzed by western blotting and immunofluorescence analysis, before and after treatment with different concentrations of 5-Aza-dC (5, 10, 20, 40 and 60 $\mu$M/l) for 48 h. (A) *GALC* protein expression was absent in the control group but present in the cells treated with different concentrations of 5-Aza-dC. β-actin protein was used as a positive control. (B) Immunofluorescent staining for *GALC* (red) and DAPI (green, nuclei). The inset is a high-magnification view. Scale bars, 50 $\mu$m. 5-Aza-dC, 5-Aza-2'-deoxycytidine.

for 24 h, the number of cells that migrated to the lower side was significantly lower in the treatment groups than in the control group ($P<0.01$). In addition, the number of the cells that migrated to the lower side was lower in the 20 $\mu$M/l group than that in the 40 $\mu$M/l group, although the difference was not statistically significant ($P>0.05$; Fig. 8).

## Discussion

Latent EBV infection is one of the most important factors for NPC in endemic areas. The transcription of EBERs is present in most NPC tumors (1-3). In the present study, no EBER expression was found in the columnar epithelial of the

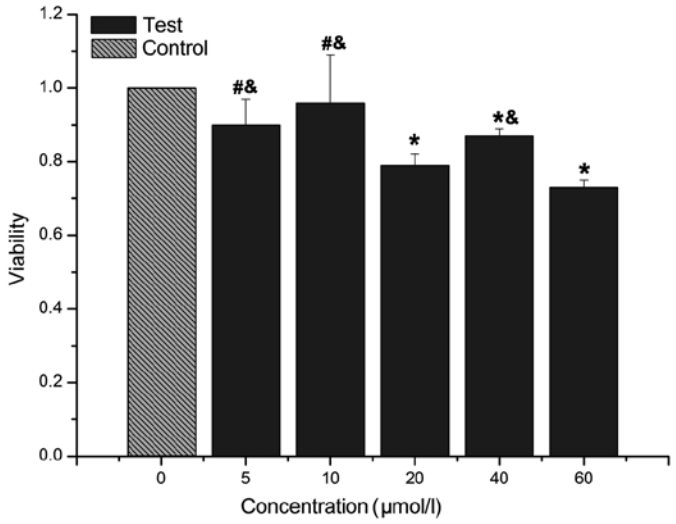


Figure 6. Viability of CNE-2Z cells treated with different concentrations of 5-Aza-dC for 48 h was determined using CCK-8 assay. Statistical analysis was performed by one-way ANOVA, followed by the least significant difference (LSD) test. Data presented as means ± SD, n=3. *P<0.05, 20, 40 and 60 $\mu$M/l vs. control. #P<0.05, 5 and 10 $\mu$M/l vs. 20 $\mu$M/l. &P<0.05, 5, 10 and 40 $\mu$M/l vs. 60 $\mu$M/l. 5-Aza-dC, 5-Aza-2'-deoxycytidine.

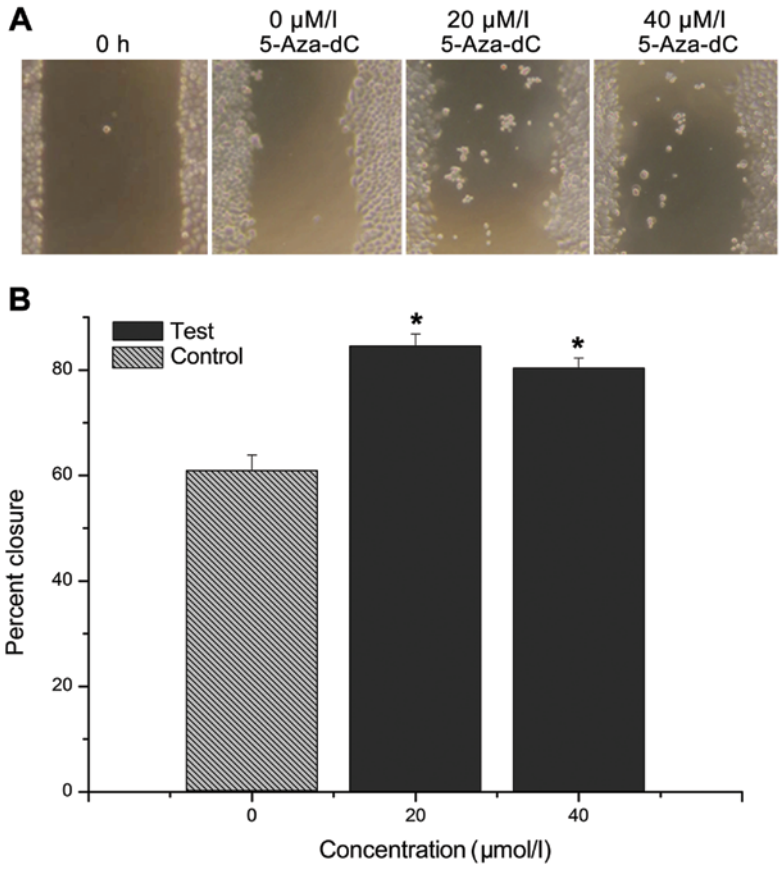


Figure 7. (A) Scratch assay was used to detect the migration of CNE-2Z cells treated with different concentrations of 5-Aza-dC for 24 h. Representative images of the cellular migration distance are shown with an original magnification of x40. (B) Statistical analysis was performed by one-way ANOVA, followed by the significant difference (LSD) test. Data presented as means ± SD, n=3. *P<0.01, 20 and 40 $\mu$M/l vs. control. 5-Aza-dC, 5-Aza-2'-deoxycytidine.

nasopharyngeal mucosa obtained from the 15 individuals in the control group. By contrast, 92.68% of the NPC specimens from the 41 NPC patients exhibited EBER expression. The immunohistochemical SP method was used to measure the expression of GALC protein. GALC protein expression was detected in 24.39% of NPC specimens, which had a high rate of EBV latent infection. GALC protein expression was detected in 60.00% of columnar epithelial of chronic nasopharyngitis specimens which had no EBV latent infection. The difference between these two groups was

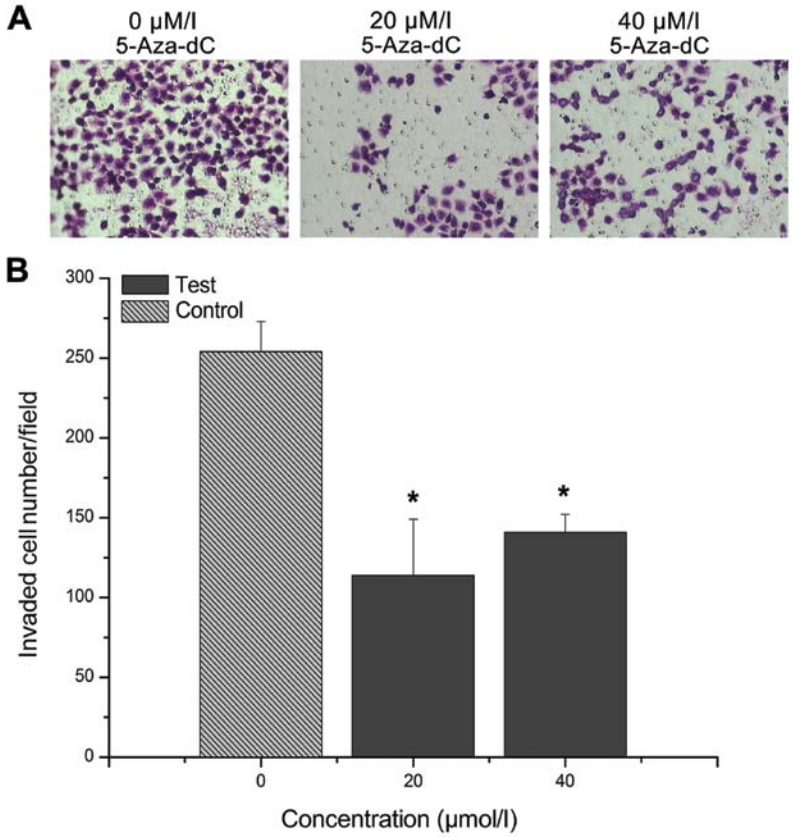


Figure 8. (A) Transwell chamber assay was used to detect the migration of CNE-2Z cells treated with different concentrations of 5-Aza-dC for 24 h. Representative images of H&E staining cells are shown with an original magnification of x200. (B) Statistical analysis was performed by one-way ANOVA, followed by the significant difference (LSD) test. Data presented as means ± SD, n=3.*P<0.01, 20 and 40 $\mu$M/l vs. control. 5-Aza-dC, 5-Aza-2'-deoxycytidine.

statistically significant (P<0.05). Subsequently, the 41 NPC specimens were divided into a lymph node metastasis and non-lymph node metastasis groups according to the TNM stage. Statistical analyses showed that the rates of the GALC protein expression were 13.79 and 50.00%, respectively, in these two groups and the difference was statistically significant (P<0.05). Logistic regression showed that the expression of GALC protein was a protective factor against lymph node metastasis of NPC (P<0.05). Compared with the normal columnar epithelial of the nasopharyngeal mucosa, the NPC cells showed a decreased expression of GALC protein. The results of the present study were in accordance with the results reported by Görögh for laryngeal squamous cell carcinoma as compared with the corresponding normal mucosa (16). The findings of the present study suggested that the downregulation of GALC protein expression in the NPC cells may be associated with EBV latent infection and the lymph node metastasis of NPC.

A study on EBV$^+$ gastric carcinoma has suggested that EBV-infected cells acquire extensive methylation that silences multiple tumor-suppressor genes and rapidly transforms into cancer cells, without going through a precancerous stage of EBV infection or methylation accumulation (17). EBV$^+$ gastric cancers show distinct methylation patterns that are likely attributable to EBV infection (18). The host defense system induces aberrant methylation in the host cellular genome (18). The host cells themselves have a methylation mechanism and, besides EBV infection, also triggers high methylation epigenotype, although this may be rare and in most cases is triggered by EBV infection (19).

LOH on chromosome 14q is detected in 80% of NPC tumors, with high-frequency LOH loci clustered at 14q11-q13,14q21-q24 and 14q32, while no LOH has been found at 14q31 (5). The *GALC* gene is located at 14q31, has 17 exons and 16 introns of ~60 kb. The deficiency of galactocerebrosidase (GALC) leads to the accumulation of psychosine, which is responsible for globoid cell leukodystrophy (Krabbe disease) in humans and certain animals. This enzyme catalyzes the lysosomal hydrolysis of specific galactolipids, including galactosylceramide (galactocerebroside) and galactosylsphingosine (psychosine). The 5'-untranslated region is GC-rich, containing no perfect CAAT or TATA sequences (6). Neither mutation nor other alterations of the *GALC* gene promoter sequence have been detected (16). Since the *GALC* gene is located at 14q31, no LOH has been found at 14q31 and neither mutation nor other alterations of the *GALC* gene promoter sequence have been detected. Therefore, we speculated that the *GALC* gene in NPC may be a tumor-suppressor gene, and downregulation of GALC protein may be associated with *GALC* gene promoter hypermethylation. Methylation of CpG sites is reversible with pharmacological demethylation using epigenetic agents such as 5-Aza-dC. Demethylation induced re-activation and expression of the genes. The NPC CNE-2Z cell line was EBV$^+$ when it was established and now, after many years of *in vitro* culture, the CNE-2Z cell line is EBER$^-$ and LMP1$^-$. In the present study, we found that the CNE-2Z cell line exhibits a low level GALC

mRNA expression and does not express GALC protein. In addition, hypermethylation (95.9%) was found at the CpG sites of the *GALC* gene promoter in the CNE-2Z cell line. Treatment and control groups were used in the present study. The CNE-2Z cells in the control group were cultured for 48 h, while the cells in the treatment groups were treated with different concentrations (5, 10, 20, 40 and 60 $\mu$M/l) of 5-Aza-dC for 48 h. Then, the GALC mRNA and protein expression, *GALC* gene promoter methylation, and cell viability in each group were measured. In addition, the migration ability of the cells in the control group and the 20 and 40 $\mu$M/l treatment groups were also measured. The results showed that compared with the control group, the treatment groups showed a significantly lower rate of promotor methylation at the CpG sites in the *GALC* gene, and these differences were more pronounced in the 20, 40 and 60 $\mu$M/l treatment groups. The expression of *GALC* mRNA was significantly higher in the treated than in the control groups ($P<0.05$), and the expression in the 20 $\mu$M/l treated group was the highest, which was significantly different from that in the other groups ($P<0.01$). GALC protein expression was detected in all the treatment groups but not in the control group. Compared with the control group, the cell viability in the 20, 40 and 60 $\mu$M/l treatment groups was significantly lower ($P<0.05$), suggesting that the cell proliferation ability decreased following treatment. The scratch assay showed that the migration distance of the cells in the 20 and 60 $\mu$M/l treatment groups was significantly higher and the cell-migration ability was significantly lower than the corresponding values in the control group ($P<0.01$). The difference between the 20 and 60 $\mu$M/l treatment groups was not statistically significant ($P>0.05$). Transwell chamber assay showed that significantly fewer cells migrated to the lower side in the 20 and 60 $\mu$M/l treatment groups than in the control group ($P<0.01$). The cell migration ability was also significantly lower in the treatment groups. The difference between the 20 and 60 $\mu$M/l treatment groups was not statistically significant ($P>0.05$). These findings demonstrated that the silencing of the *GALC* gene in the CNE-2Z cells was closely associated with the hypermethylation of the CpG sites in the promoter, while demethylation effectively inhibited the proliferation and migration of the CNE-2Z cells. The results of the present study were in accordance with previous findings (20,21).

Experiments on DNA methylation of cancer-related genes have suggested that promoter hypermethylation is a potential biomarker for the early diagnosis and a therapeutic target in cancer (12-14). We report that *GALC* is downregulated in NPC, and that promoter hypermethylation contributes to the loss of *GALC* expression. To the best of our knowledge, this is the first study demonstrating *GALC* gene promoter hypermethylation in NPC. Our functional studies support the putative tumor-suppressor effect of *GALC* in the NPC CNE-2Z cell line. The present findings suggest that *GALC* gene promoter hypermethylation is a potential epigenetic biomarker for the early diagnosis and prediction of metastasis of EBV-associated NPC.

## Acknowledgements

This study was supported by the National Basic Research Program of China (973 Program, no. 2011CB504800), and the 2013 Scientific Research Foundation of Guangdong Medical University, Zhanjiang, China (no. M2013033).

## References

1. Young LS and Dawson CW: Epstein-Barr virus and nasopharyngeal carcinoma. Chin J Cancer 33: 581-590, 2014.
2. Busson P, Keryer C, Ooka T and Corbex M: EBV-associated nasopharyngeal carcinomas: From epidemiology to virus-targeting strategies. Trends Microbiol 12: 356-360, 2004.
3. Tao Q, Young LS, Woodman CB and Murray PG: Epstein-Barr virus (EBV) and its associated human cancers - genetics, epigenetics, pathobiology and novel therapeutics. Front Biosci 11: 2672-2713, 2006.
4. Lo KW, Teo PM, Hui AB, To KF, Tsang YS, Chan SY, Mak KF, Lee JC and Huang DP: High resolution allelotype of microdissected primary nasopharyngeal carcinoma. Cancer Res 60: 3348-3353, 2000.
5. Shao J, Li Y, Wu Q, Liang X, Yu X, Huang L, Hou J, Huang X, Ernberg I, Hu LF, *et al*: High frequency loss of heterozygosity on the long arms of chromosomes 13 and 14 in nasopharyngeal carcinoma in Southern China. Chin Med J 115: 571-575, 2002.
6. Luzi P, Rafi MA and Wenger DA: Structure and organization of the human galactocerebrosidase (GALC) gene. Genomics 26: 407-409, 1995.
7. Kwong J, Lo KW, To KF, Teo PM, Johnson PJ and Huang DP: Promoter hypermethylation of multiple genes in nasopharyngeal carcinoma. Clin Cancer Res 8: 131-137, 2002.
8. Tong JH, Tsang RK, Lo KW, Woo JK, Kwong J, Chan MW, Chang AR, van Hasselt CA, Huang DP and To KF: Quantitative Epstein-Barr virus DNA analysis and detection of gene promoter hypermethylation in nasopharyngeal (NP) brushing samples from patients with NP carcinoma. Clin Cancer Res 8: 2612-2619, 2002.
9. Challouf S, Ziadi S, Zaghdoudi R, Ksiaa F, Ben Gacem R and Trimeche M: Patterns of aberrant DNA hypermethylation in nasopharyngeal carcinoma in Tunisian patients. Clin Chim Acta 413: 795-802, 2012.
10. Tong JH, Ng DC, Chau SL, So KK, Leung PP, Lee TL, Lung RW, Chan MW, Chan AW, Lo KW, *et al*: Putative tumour-suppressor gene *DAB2* is frequently down regulated by promoter hypermethylation in nasopharyngeal carcinoma. BMC Cancer 10: 253, 2010.
11. Bodoor K, Haddad Y, Alkhateeb A, Al-Abbadi A, Dowairi M, Magableh A, Bsoul N and Ghabkari A: DNA hypermethylation of cell cycle (p15 and p16) and apoptotic (p14, p53, DAPK and TMS1) genes in peripheral blood of leukemia patients. Asian Pac J Cancer Prev 15: 75-84, 2014.
12. Park JY: Promoter hypermethylation as a biomarker in prostate adenocarcinoma. Methods Mol Biol 1238: 607-625, 2015.
13. Wang HL, Zhou PY, Liu P and Zhang Y: Role of *p16* gene promoter methylation in gastric carcinogenesis: A meta-analysis. Mol Biol Rep 41: 4481-4492, 2014.
14. Gloss BS, Patterson KI, Barton CA, Gonzalez M, Scurry JP, Hacker NF, Sutherland RL, O'Brien PM and Clark SJ: Integrative genome-wide expression and promoter DNA methylation profiling identifies a potential novel panel of ovarian cancer epigenetic biomarkers. Cancer Lett 318: 76-85, 2012.
15. Wei KR, Xu Y, Liu J, Zhang WJ and Liang ZH: Histopathological classification of nasopharyngeal carcinoma. Asian Pac J Cancer Prev 12: 1141-1147, 2011.
16. Görögh T, Rudert H, Lippert BM, Gottschlich S, Maune S, Heidorn K, Maass J, Hoffmann M, Meyer JE, Rathcke IO, *et al*: Transcriptional repression of the human galactocerebrosidase gene in squamous cell carcinomas of the larynx. Int J Cancer 83: 750-754, 1999.
17. Kaneda A, Matsusaka K, Aburatani H and Fukayama M: Epstein-Barr virus infection as an epigenetic driver of tumorigenesis. Cancer Res 72: 3445-3450, 2012.
18. Matsusaka K, Kaneda A, Nagae G, Ushiku T, Kikuchi Y, Hino R, Uozaki H, Seto Y, Takada K, Aburatani H, *et al*: Classification of Epstein-Barr virus-positive gastric cancers by definition of DNA methylation epigenotypes. Cancer Res 71: 7187-7197, 2011.
19. Fukayama M, Hino R and Uozaki H: Epstein-Barr virus and gastric carcinoma: Virus-host interactions leading to carcinoma. Cancer Sci 99: 1726-1733, 2008.
20. Owczarek TB, Suchanski J, Pula B, Kmiecik AM, Chadalski M, Jethon A, Dziegiel P and Ugorski M: Galactosylceramide affects tumorigenic and metastatic properties of breast cancer cells as an anti-apoptotic molecule. PLoS One 8: e84191, 2013.
21. Beier UH and Görögh T: Implications of galactocerebrosidase and galactosylcerebroside metabolism in cancer cells. Int J Cancer 115: 6-10, 2005.